Amphiphilic Diblock Copolymers on Mica: Formation of Flat Polymer Nanoislands and Evolution to Protruding Surface Micelles

Emmanouil Glynos,[†] Stergios Pispas,[‡] and Vasileios Koutsos*,[†]

Institute for Materials and Processes, School of Engineering and Electronics & Centre for Materials Science and Engineering, University of Edinburgh, King's Buildings, Edinburgh EH9 3JL, United Kingdom, and Theoretical and Physical Chemistry Institute, National Hellenic Research Foundation, 48 Vass. Constantinou Ave., 11635 Athens, Greece

Received November 27, 2007; Revised Manuscript Received April 1, 2008

ABSTRACT: We show that the deposition of poly(isoprene-*b*-ethylene oxide) block copolymer (PI−PEO) micelles on freshly cleaved mica produced ultraflat, polymer nanoislands of well-defined monomolecular thickness. The islands were partly adsorbed and partly floating on the substrate, and their morphology changed over time (under ambient conditions). Their structural evolution was recorded and analyzed using atomic force microscopy. Larger islands evolved to high globular aggregates while smaller islands behaved in distinctly different manner becoming shorter; in both cases, the final structures had a surface micelle shape and organization. The time-dependent behavior originates from a decrease of the amount of water adsorbed to the mica surface, due to the fact that freshly cleaved mica under ambient conditions changes its surface character from highly hydrophilic to less hydrophilic with increasing exposure time. The combination and competition of strong affinity of the PEO block with the adsorbed water and flexibility of the hydrophobic PI block results in the formation and evolution of these supramolecular structures.

Introduction

Block copolymers have received considerable attention as the building blocks for bottom-up, self-assembled nanostructures[1] which can be used in a variety of enabling nanotechnologies[2] associated with a diverse number of applications. In particular, thin and ultrathin films of block copolymers[3] promise unique solutions for various technology sectors spanning from biotechnology[4] to nanoelectronics.[5] Unique opportunities for modifying surfaces to achieve tunable properties arise if one uses appropriate block copolymer nanostructures responsive to certain external stimuli such as pH,[6,7] annealing, and exposure to solvents.[8]

Block copolymer nanostructures adsorbed and/or self-assembled on solid surfaces have been extensively studied by atomic force microscopy (AFM)[7,9–25]—a technique which offers unprecedented spatial resolution and real space images in three dimensions. The vast majority of these studies are concerned with stable equilibrium structures of multichain aggregates and supramolecular assemblies, in solution or more usually in dry state, which in many cases take the form of stripelike or spherically shaped micellar structures.[18,25] Diblock copolymers form spherical micelles in a solution (for concentrations above the critical micelle concentration, cmc) within a selective solvent[26,27] and in many cases could remain more or less intact after deposition on a solid substrate.[23] Alternatively, *surface micelles* can be formed due to the selective adsorption of one of the two blocks onto the substrate forming a thin monolayer while the other blocks aggregate on top or in this layer forming spherically shaped domes.[9,22,24,28] Amphiphilic block copolymers consisting of a hydrophobic and a hydrophilic block have attracted considerable interest lately, owing to their ability to form micelles *in water*—a crucial property for biomedical and environmental applications.[29,30] Micelle surface relaxation, reorganization, spreading, and some partial *dissociation* have been reported in the case of hydrophobic substrates which attract the hydrophobic micellar core.[23,24,28,31]

In this study we show that (a) *the presence* of an ultrathin surface water film can instigate the formation of flat, polymer, brushlike islands of well-defined thickness which are sensitive to the surface conditions and (b) *the progressive depletion* of the ultrathin water film can induce the structural evolution of these flat islands to protruding nanostructures of surface micelle shape and organization. To our knowledge, it is the first time that these ultraflat polymer islands were observed and imaged, and their progressive evolution to surface micellar structures has been captured in real time. Furthermore, we show that there is a very important size effect and islands of different size behave in a distinctively different manner.

Of paramount importance in the interpretation of our results is the behavior of water on freshly cleaved mica in ambient conditions. Mica is one of the most usual model substrates for AFM studies of polymer nanostructures, adsorbed polymers, and biomolecules on surfaces. Clean, contamination-free, and atomically flat mica surfaces can be prepared by cleavage. However, the role of the water layer always present on mica in ambient conditions has been usually ignored in these studies. In general, a thin film of water grows on hydrophilic surfaces in ambient conditions via water vapor adsorption and condensation on the solid surface.[32,33] This is an important phenomenon as it can alter the interactions between the surface and adsorbed molecules, especially if these molecules have strong affinity with water. The amount of water adsorbed on a hydrophilic surface is determined by the environmental conditions. Mica has been proven to be a popular substrate for studying the physicochemical properties of adsorbed water layers. Freshly cleaved mica in ambient conditions adsorbs water from the atmosphere because of its high hydrophilicity, which results in an ordered or partially ordered water layer. The existence of the adsorbed water layer on mica has been established in many studies using various experimental techniques.[34–40] These studies revealed that at ambient temperature and relative humidity, RH ≈ 50%, two layers of water are formed. There is a first structured/ordered and rigid layer of water due to its strong bonding with the mica

* To whom correspondence should be addressed: Ph +44 (0)131 6508704; Fax +44 (0)131 6506551; e-mail vasileios.koutsos@ed.ac.uk.
[†] University of Edinburgh.
[‡] National Hellenic Research Foundation.

10.1021/ma702630c CCC: $40.75
Published on Web 05/29/2008

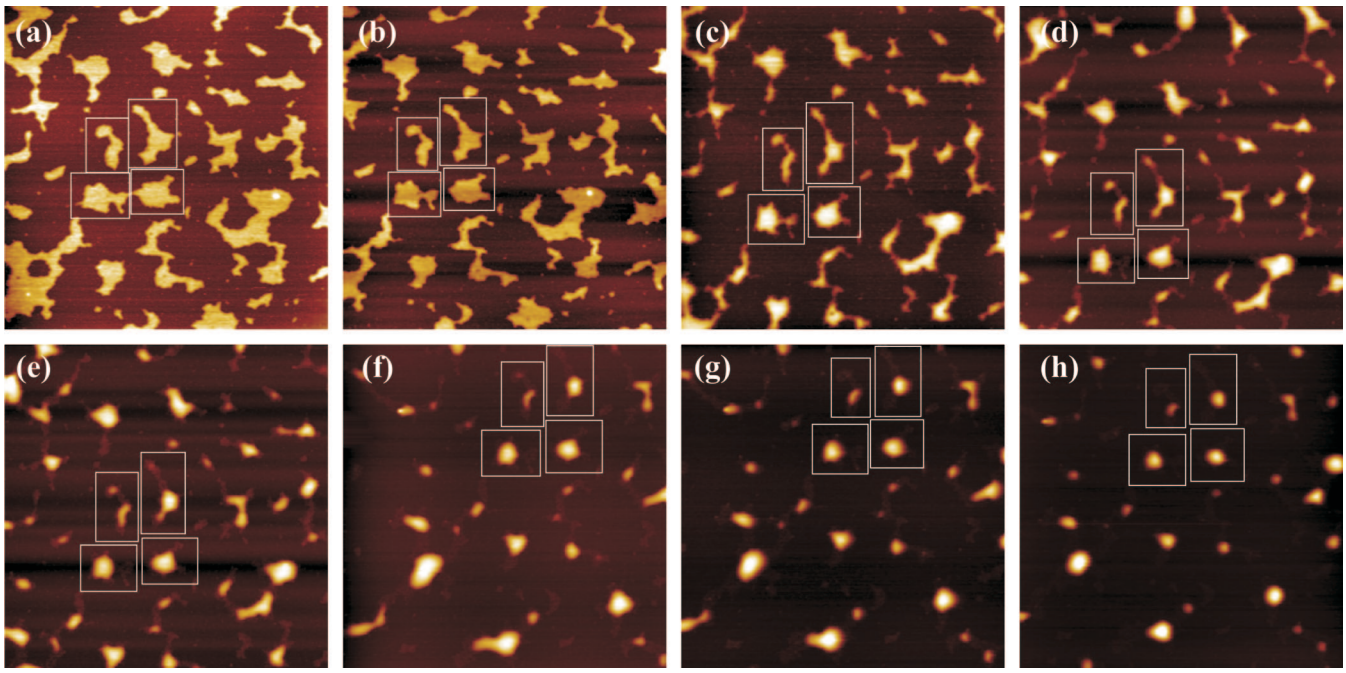

Figure 1. Tapping mode AFM height images (3.66 × 3.66 μm^2) of nominally the same area after (a) 89, (b) 133, (c) 489, (d) 598, (e) 745, (f) 1425, (g) 1825, and (h) 2740 min from sample preparation. The top left, top right, bottom left, and bottom right inset boxes denote structures A, B, C, and D, respectively.

surface, which has been denominated *phase I* by Hu and coworkers;[35,36] its thickness has been estimated to be of molecular dimensions (≈0.2 nm). Hu et al.[35,36] used controlled environmental conditions and found that the formation of the phase I was complete at RH ≈ 22%−28%. The existence of this bound and rigid phase I has been also verified by molecular dynamics simulations.[41,42] Above the phase I there is a second thicker bulklike layer of water which has been called *phase II*.[35,36] Both layers have been observed to form immediately after cleavage, showing that the adsorption of water happens rapidly. Phase II thickness can vary from one monolayer of water to ≈2 nm[35–37,40] and can take the form of asymmetric islands.[35,36,38] In any case, it is clear that the second layer is connected through hydrogen bonds to the first layer, resulting in a liquid-structured layer with properties of bulk water (under ambient conditions). A characteristic property of mica surfaces is that they become less hydrophilic in time; in ambient conditions this is a gradual process and can take a few days.[38] This results possibly from the accumulation of contaminant materials of organic origin always present in ambient conditions.[36,38] This change results in a gradual removal of phase II, as the water molecules cannot H-bond with the structured phase I. Thus, progressively with time, the amount of water absorbed on mica, mainly of phase II, decreases.

The fact that the mica water layer influences the behavior of adsorbed molecules in ambient conditions has been reported recently.[43–45] Kumaki et al.[46] deposited poly(styrene)-*block*-poly(methyl methacrylate), PS−PMMA, diblock copolymers on mica by the Langmuir−Blodgett (LB) method using small surface pressure during deposition, to achieve isolated molecules of PS−PMMA. The sample preparation methodology was similar to the one used in previous studies to obtain single-chain PS particles.[47,48] By imaging the samples with AFM in their laboratory ambient conditions, 50−60% RH, they found changes of the single polymer conformation on mica with time and the formation of aggregations of a few PS−PMMA molecules. These small aggregates appeared with a core consisting of few assembled PS blocks surrounded by extended PMMA blocks. They argued that the decrease of the water layer thickness made the PMMA blocks to laterally expand and the whole structure to appear shorter. It has to be noted that although PMMA is not a water-soluble molecule, it can interact with water due to attractive interactions of the $-COOCH_3$ groups with water.

In our work, amphiphilic diblock copolymer micelles of poly(isoprene-*b*-ethylene oxide) block copolymer (PI−PEO), which consists of a short and very flexible hydrophobic block (PI) and a long hydrophilic block (PEO), were deposited on mica, resulting in the formation of ultraflat supramolecular islands which evolved structurally to polymer globules of spherical cap shape and surface micelle organization as mica became less hydrophilic with time.

Experimental Section

Synthesis and Characterization of the PI−PEO Block Copolymer. The poly(isoprene-*b*-ethylene oxide) block copolymer (PI−PEO) was synthesized by anionic polymerization high-vacuum techniques. Monomers and solvent were purified to the standards of anionic polymerization using well-established purification techniques.[30,49,50] Polymerizations were conducted in benzene using *sec*-butyllithium (*sec*-BuLi) as the initiator. Isoprene was polymerized first at room temperature. The resulting polyisoprene (PI), under these experimental conditions, has a high percentage of 1,4 microstructure (∼92% as determined by ^1H NMR spectroscopy). After completion of the polymerization of the first monomer, the predetermined amount of purified ethylene oxide was added in the polymerization mixture. The color of the solution changed immediately from pale yellow to colorless due to the crossover reaction from living polyisoprenyllithium (PILi) to polyisoprene−ethylene oxide lithium (PI−EOLi). Under these conditions only one ethylene oxide unit is added to the PILi chain end, since anionic polymerization of ethylene oxide by Li as the counterion is not possible.[49] A predetermined amount of phosphazine base, as a solution in hexane, was subsequently added (phosphazine:Li = 0.9:1 molar ratio).[30,51,52] The temperature of the solution was subsequently raised to 40 °C, and the reaction mixture was left for 2 days for completion of ethylene oxide polymerization. Active chain ends were deactivated with degassed methanol in the presence of a small amount of HCl. The polymers were precipitated in acetone,

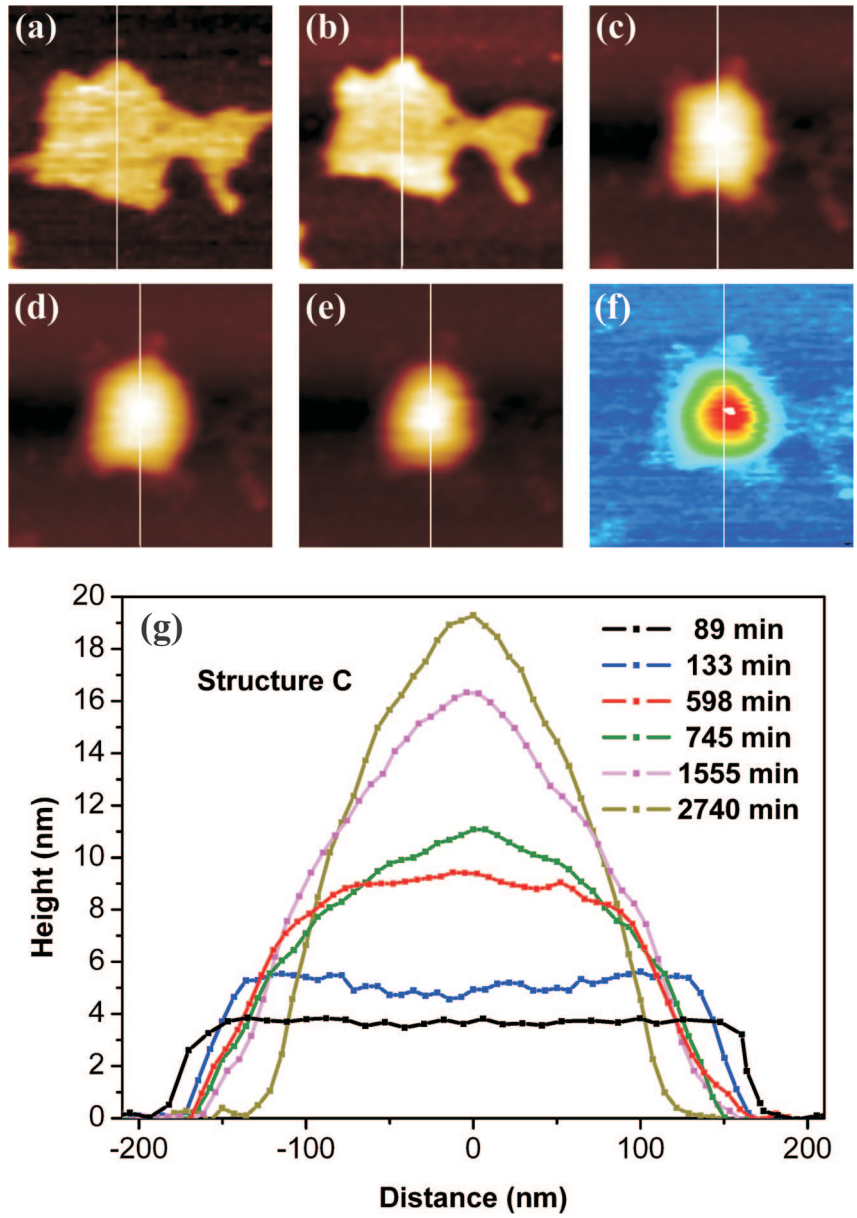

Figure 2. AFM height images (0.6 × 0.6 μm^2) of structure C for (a) 89, (b) 133, (c) 598, (d) 745, (e) 1555, and (f) (high contrast image) 2740 min after the sample was prepared with the corresponding profiles shown in (g) and indicated with the white line in each AFM image.

stabilized with 2,6-di-*tert*-butyl-*p*-cresol at −20 °C, and dried in a vacuum.

Molecular weights and molecular weight distributions of the block copolymers were determined by size exclusion chromatography (SEC) using a Waters system, composed of a Waters 1515 isocratic pump, a set of three μ-Styragel mixed bed columns, with a porosity range of 10^2-10^6 Å, and a Waters 2414 refractive index detector (at 40 °C) and controlled through Breeze software. Tetrahydrofuran was the mobile phase used at a flow rate of 1.0 mL/min at 30 °C. The setup was calibrated with polystyrene standards having weight-average molecular weights in the range 2500−900 000 g/mol. No peaks corresponding to the PI block were observed in any case leading to the conclusion that the block copolymer is free from PI homopolymer impurities. The average composition of the copolymer and microstructure of the PI block were determined by ^{1}H NMR spectroscopy using a Bruker AC 300 spectrometer in $CDCl_3$ at 30 °C. The weight-average molecular weight of the copolymer was found to be M_w = 20 700 with a molecular weight polydispersity, M_w/M_n = 1.03. The diblock copolymer contains 29 wt % PI.

Dynamic and static light scattering measurements on aqueous solutions of the block copolymer were performed on a ALV/CGS-3 compact goniometer system (ALV GmbH, Germany), using a JDS Uniphase 22 mW He−Ne laser, operating at 632.8 nm, and an avalanche photodiode detector, interfaced with a ALV-5000/EPP multitau digital correlator with 288 channels and a ALV/LSE-5003 light scattering electronics unit for stepper motor drive and limit switch control. Autocorrelation functions, from DLS measurements, were collected five times for each solution, and they were analyzed by the cumulants method and the CONTIN routine. Typically correlation functions were collected for 20 s. Fits to the correlation functions were made using the software provided by the manufacturer. A "probability one to reject" of 0.5 was used routinely in the CONTIN analysis software. Measurements were made at a scattering angle of 90° and at a temperature of 25 °C on solutions of the amphiphilic block copolymer. Apparent hydrodynamic radii, $R_{h,app}$, at different polymer concentrations were calculated by aid of the Stokes−Einstein equation, $R_{h,app} = kT/6\pi\eta_0 D_{app}$, where k is the Boltzmann constant, T the absolute temperature, η_0 the solvent viscosity, and D_{app} the diffusion coefficient calculated from the analysis of the correlation function at the particular polymer concentration. The copolymer was found to form micelles with a constant $R_h = 41 \pm 1.0$ nm, having a narrow size distribution ($\mu_2/\Gamma^2 < 0.1$, where μ_2 is the second cumulant and Γ the decay rate of

the correlation function) in the concentration range studied (2×10^{-4}−4×10^{-3} g/mL). The aggregation number of the micelles was found to be ∼1450.

For fluorescence measurements pyrene (Aldrich, recrystallized from ethyl acetate) was used as a hydrophobic probe. A pyrene solution in acetone was prepared first at a concentration of 1 mM. Fixed volumes of this solution were introduced with a micropipet in glass vials, the acetone was allowed to evaporate, and appropriate volumes of the aqueous block copolymer solutions of different concentration were introduced, in order to give a final pyrene concentration lower than 3×10^{-7} M. These solutions were allowed to equilibrate overnight and measured the next day.

Steady-state fluorescence spectra of pyrene probe in aqueous solutions were recorded with a double-grating excitation and a single-grating emission spectrofluorometer (Fluorolog-3, model FL3−21, Jobin Yvon-Spex) at room temperature (ca. 25 °C) using air-equilibrated solutions. Excitation wavelength was $\lambda = 335$ nm, and emission spectra were recorded in the region 350−500 nm, with an increment of 1 nm, using an integration time of 0.5 s. The I_1/I_3 ratio was determined as the average of three measurements (where I_1 and I_3 are the intensities of the first and the third peaks of the pyrene fluorescence spectra at 372 and 383 nm, respectively). The critical micellar concentration (cmc) for the PI−PEO micelles was found at a concentration of 1.44×10^{-5} g/mL.

Sample Preparation and AFM Measurements. The solutions were prepared by dissolving a known amount of the sample in the appropriate volume of ultrapure deionized water with resistivity of 18.2 MΩ cm. As an extra precaution, the solutions were heated at 60 °C overnight before use to ensure complete dilution of the sample.[30] The concentrations of the solutions were kept well above the cmc, around 2×10^{-3} g/mL. Before use the solution was filtered through 0.45 μm hydrophilic Teflon Millipore filters. A droplet of a deionized water solution of PI−PEO block copolymer was deposited on freshly cleaved mica (Agar Scientific, Essex, UK) for 5 min, and the sample was rinsed very gently to remove some of the solution from mica. The sample was gently dried under a stream of nitrogen. Subsequently, it was placed in a clean glass Petri dish and imaged with AFM in ambient conditions using a Veeco AFM, Multimode/Nanoscope IIIa (Veeco, Santa Barbara, CA) equipped with an E-scanner (x−y scan range: ∼14 μm). The samples were imaged in tapping mode (tip in intermittent contact with the surface). The RTESPA Veeco cantilevers with a nominal spring constant and resonance frequency of 40 N/m and 300 kHz, respectively, were used to image the samples. In general "light tapping" was used by keeping the set-point amplitude ratio $r_{sp} = A_{sp}/A_0$ close to 1 (where A_0 and A_{sp} are the free oscillation amplitude and the reduced scanning set-point amplitude of the cantilever, respectively) in order to minimize the interaction force between the tip and the substrate (but without losing contact).[53−55] The cantilevers were oscillated vertically 5% below their natural resonance frequency and moved in a raster fashion within a specified region of interest. During AFM measurements the r_{sp} was kept at about 0.9−0.95. Images were processed, and the island heights were measured using the software Scanning Probe Image Processor (SPIP, Image Metrology). In order to avoid any influence of the sample from the laser (e.g., temperature increase) or any capillary necking events between the tip and the sample, the laser was switched off and the tip was retracted few micrometers during the time between consecutive scans.

Results and Discussion

In the series of experiments presented here (at RH ≈ 55% and $T \approx 21$ °C), the first measurement was obtained 89 min after the sample was prepared and the last after 3240 min. Figure 1 shows AFM images of polymer-modified mica substrates taken from 89 min up to 2740 min after sample preparation. We can clearly see several irregular islands (some of them still connected together in the first image) developing into almost circular domains. AFM images were taken also for 2980 and 3240 min, but no significant changes were observed for both the lateral

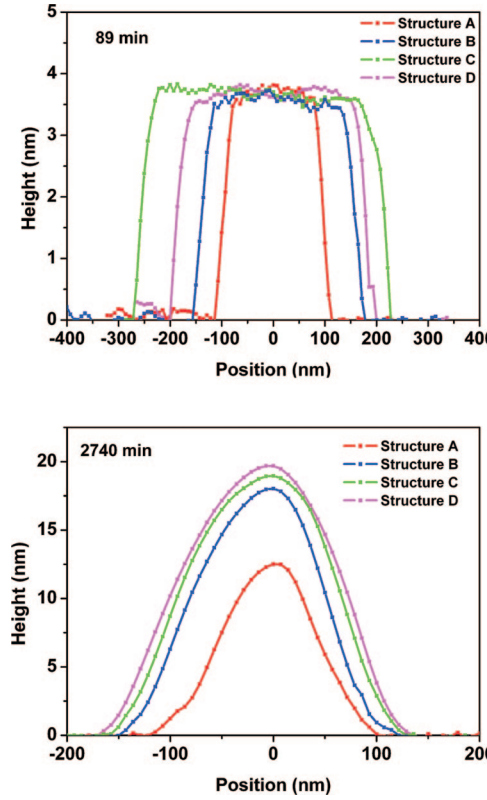

Figure 3. Horizontal profiles of structures A (red), B (blue), C (green), and D (purple) for 89 min (top) and 2740 min (bottom) after the sample was prepared.

and vertical dimensions of the islands, indicating that the structures had reached a steady state. Between scans the tip was retracted a short distance from the mica substrate, and upon the reapproach, short displacements of the area of interest were observed. These displacements on the images originate from thermal drifts and hysteretic behavior of the piezocrystal scanner. Hence, few islands were present in all captured images. Four of these structures are indicated by the white boxes in Figure 1. For simplicity, from now on we will refer to these islands as structures A, B, C, and D for the islands in the top left box, top right box, bottom left box, and bottom right box, respectively.

By zooming-in on a typical island more details of the structural evolution can be seen (Figure 2). Satellite substructures in the periphery of the main islands and smaller isolated islands evolved with time in a distinctively different manner (became shorter and almost "disappeared" with time). We will now concentrate on the time evolution of the large structures and the behavior of the satellite substructures, and small structures will be discussed later. In parts a, b c, d, e, and f of Figure 2, AFM image snapshots of the time evolution of structure C are shown for 89, 133, 598, 745, 1555, and 2740 min after the sample preparation, respectively. Vertical profiles along the white line in each AFM image are plotted in Figure 2g. With time the polymeric island shrank laterally and expanded vertically taking the shape of a spherical cap. The profiles ultimately appear to be higher by a factor of almost 5 while the shape narrows progressively. It can be clearly seen that while the height changes dramatically (∼500%) the width changes only weakly (maximum of ∼40%). This is not surprising since it is well-known that AFM images are always a "convolution" of the geometry of the tip and the shape of the imaged object. For geometrical reasons, higher objects "suffer" more from the convolution effect, and their width is much more overestimated. As has been reported in AFM studies on single molecules/particles, the convolution effect generally overestimates the

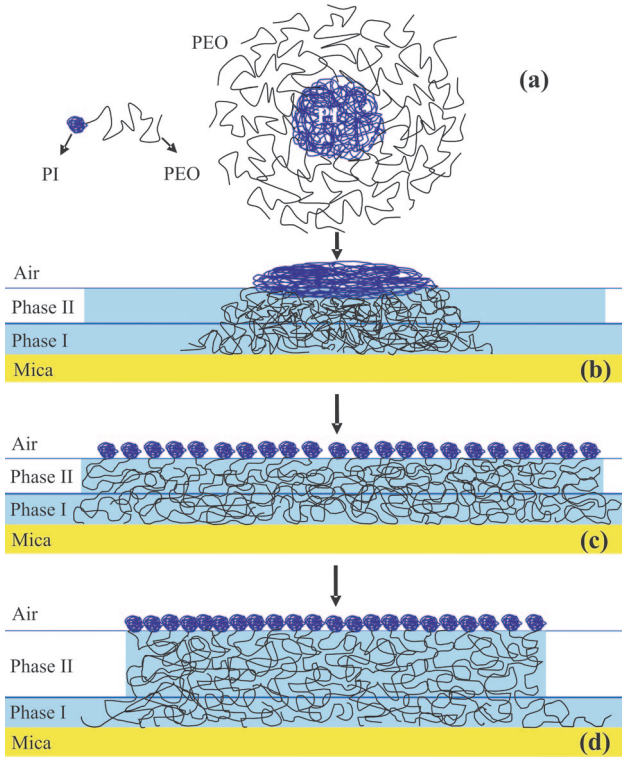

Figure 4. (a−c) Schematic drawing of the deformation and dissociation of a deposited PI−PEO micelle on a freshly cleaved mica forming a flat brushlike polymeric island within a phase II water layer. (d) Initial stage of the confinement of the polymers within narrower phase II water islands. The swelling of the PEO block is exaggerated especially at the vertical direction for illustration reasons.

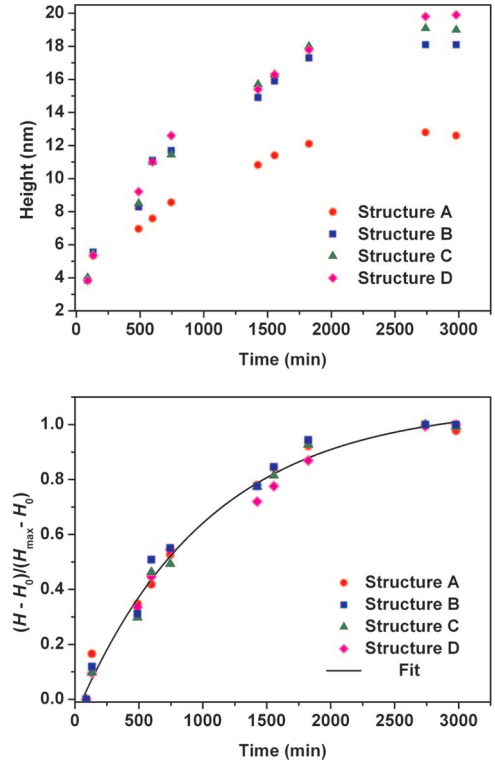

Figure 5. (top) Height of the island against time and (bottom) normalized height increase vs time for structures A (red circles), B (blue squares), C (green triangles), and D (pink diamonds) with the corresponding exponential-type fit, $(H - H_0)/(H_{max} - H_0) = a(1 - be^{-ct})$ with $\alpha = 1.072$, $b = 1.059$, and $c = 0.001$ min^{-1}.

lateral dimensions of the object while the height is much more realistic.[56] In the last high contrast image (Figure 2f) it can be clearly seen that a very thin layer (≈0.4 nm) has remained around the central protruding structure.

In Figure 3 (top) horizontal profiles of structures A, B, C, and D measured 89 min after sample preparation, when phase II water is present, show that all structures were flat with identical heights of ∼3.7 nm, even though they do not have the same lateral dimensions. In the final state shown in Figure 3 (bottom), when phase II water has disappeared, all structures increased their height and attained similar spherical cap shapes. It is important to note that the final height depends on the overall initial volume of the supramolecular structure and that larger islands resulted in higher final spherical cap shaped globules.

The concentration of the solution used for the sample preparation was above the cmc; hence, the diblock copolymers were organized into micelles of PI core and a PEO corona. Contrary to other micelle structure observations on surfaces reporting spherically shaped micelles and "domes" (in good and in bad solvent conditions),[7,9–11,18,19,22–24] in our case the initial structures were flat asymmetric islands of identical height. As has already been discussed in the Introduction, phase II can be envisaged as an ultrathin layer of water with high mobility that can take the form of asymmetric islands. Immediately after our gentle deposition and drying, we expect to have the polymeric micelles within the water film of phase II. The flat islands of identical height observed in the beginning of the process indicate that the micelles were dissociated and formed a flat polymer structure. The reason for this behavior is encoded within the physicochemical characteristics of the diblock copolymer used. It contains 71 wt % PEO, resulting in a water-soluble corona as the dominant part of the micelle. The PI blocks of the molecules forming the core are relatively short with a molecular weight of 6 kg/mol. Krishnamoorti et al.[57] measured the entanglement molecular weight (M_e) for PI to be 6.37 kg/mol. Thus, in our case the molecular weight of the PI block is smaller than M_e, and hence we do not expect a significant number of entanglements between the PI chains in the core. Moreover, at room temperature the PI is expected to be liquidlike since its glass transition temperature (T_g) is −67 °C (or even lower as the T_g of thin polymer films might be below its bulk value[58]). Furthermore, studies showed that polystyrene-*block*-poly(2-vinylpyridine)-*block*-poly(ethylene oxide), PS−PVP−PEO, micelles with small PS cores are soft and deformed after deposition on mica[59] while polystyrene-*block*-poly(methacrylic acid), PS−PMA, micelles with larger PS cores deposited on mica appeared stiff and did not deform.[60] Hence, it is reasonable to expect that the much more flexible PI−PEO micelles of our study could *readily deform*, and since they are *amphiphilic* and had to be *confined* within the water layer on mica, their complete dissociation was energetically favored. We expect that the PI block concentrated at the air−phase II water interface while the water-soluble PEO block expanded within the water layer. This behavior is shown schematically in Figure 4. The unusual nature of the observed islands is that they are partly adsorbed (in the sense that they are confined within the ultrathin water layer via the hydrophilic PEO block) and partly floating (due to their amphiphilic character). The larger PEO block is swollen but confined within the water islands of phase II on mica and the smaller PI block collapsed at the water−air interface (Figure 4). The initial heights of these islands are consistent with the molecular dimensions of a single PI−PEO molecule (in the range of few nanometers).

During the exposure of mica to ambient conditions, the phase II water on mica was disappearing as the mica became less hydrophilic with time. Therefore, gradually the PEO blocks were confined further within a narrower phase II water layer. During

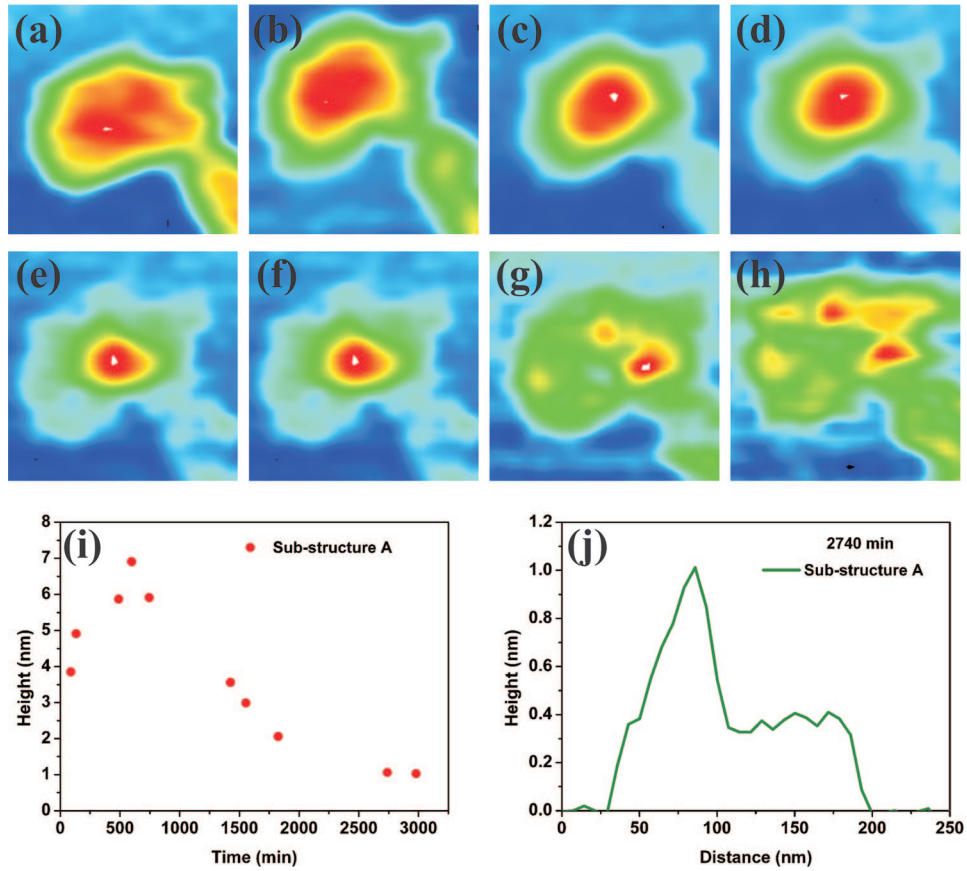

Figure 6. High-contrast AFM images for the case of the secondary substructure in structure A after (a) 133, (b) 489, (c) 598, (d) 745, (e) 1425, (f) 1555, (g) 1825, and (h) 2740 min since the sample was prepared; (i) plot of the corresponding maximum height evolution of the substructure: the height initially increased but later decreased; (j) a height profile of the substructure taken from an AFM image after 2740 min since the sample was prepared showing a maximum height of about 1 nm but also flat areas of about 0.4 nm.

the initial stages the islands remained flat, and consequently their vertical expansion could be associated with the steric repulsions between the PEO blocks as a gradually denser polymer brush was forming. The aggregation was aided by the attractive interactions of the small and flexible PI blocks. The parts of the PEO blocks which could not be accommodated within the phase I water layer passed from good-solvent conditions (characterized by steric repulsions) to bad-solvent conditions (characterized by attractive interactions), enhancing further the formation of a spherical cap aggregate. The low height (≈0.4 nm) layer surrounding the central globular aggregate can be associated with the laterally extended PEO blocks within the phase I water on mica which oppose the aggregation process. It is therefore clear that some of (or parts of) the hydrophilic PEO blocks did not follow the aggregation process but extended laterally and adopted flat conformations within/on the remaining phase I layer of water. This is the same dimensions and due to the same physics as the intercalated PEO structures when PEO is inserted in hydrated mica-type layered silicates forming industrially significant nanocomposite materials which have been studied extensively both experimentally and by computer simulations.[61–69] The height of these areas, ≈0.4 nm, is also consistent with AFM measurements of the thickness of extended adsorbed polymer coils (e.g., 0.4 nm for poly(2-vinylpyridine), P2VP, chains on mica).[70] The width of PEO chains has similar sizes as inferred by scattering and diffraction techniques.[71,72] Hence, the overall structure in the final stage is reminiscent of a large *surface micelle*. As already mentioned, the width and consequently the volume of the structures is overestimated in AFM images due to the tip convolution effect. Using a methodology based on simple geometrical arguments and described in detail in our recent paper,[73] we estimated the volume of the polymer islands at the latest stages of evolution (so that they are not affected/swollen by the water) to be few times larger than the volume of a "dry" micelle, $\sim 0.5 \times 10^5$ nm^3, calculated from the micelle aggregation number and assuming bulk polymer densities. For example, the deconvoluted volume of the central high feature (alone) of structure D is $\approx 2 \times 10^5$ nm^3. These values suggest that the large structures were the product of dissociation of few to several individual micelles within the asymmetric islands of phase II.

In Figure 5 (top), the height is plotted against time for each structure, and it can be clearly seen that the height evolution for all structures shows similar behavior. The height converges to a specific plateau value after a long time, 2740 min, indicating that the observed shape evolution was terminated. In Figure 5 (bottom), the ratio of the height increase ($H - H_0$, where H and H_0 are the instantaneous and the initial height, respectively) over the maximum height (H_{max}) increase of each structure ($H_{max} - H_0$) is plotted against time, and the data are fitted with a generic exponential-type function $(H - H_0)/(H_{max} - H_0) = a(1 - be^{-ct})$, where a, b, and c are fitting parameters. It is clear that for all large structures the evolution has the same behavior. The kinetics of the time evolution is expected to be complicated and to be affected by several processes such as the hydrophilicity changes of mica, the mobility of the PEO blocks within the water layer, and the viscoelastic response of the polymers.

In Figure 6a−h, we show high-contrast AFM images of the small satellite substructure of structure A. Other small satellite substructures and isolated islands of the same (small) size have very similar behavior. The height evolution of this substructure (Figure 6i) shows that its (maximum) height

increased up to 598 min and then decreased. At the beginning, i.e. 89 min after the sample was prepared, this particular feature appeared with similar height as the other structures, i.e. around 3.8 nm. In the end, 2740 min after the sample was prepared the substructure was shorter with a maximum height of ~1 nm. The AFM image profile for this case (Figure 6j) shows that this feature appeared with a bimodal conformation as there are areas with height of ~1 nm, corresponding to the red regions of the high-contrast AFM image, and a wider area with height around 0.4 nm, corresponding to the green region. This behavior is similar to the behavior of single PS−PMMA molecules on mica.[46] It seems that in the case of small islands the behavior is dominated by the *small number* of large hydrophilic PEO blocks: all of them extended laterally and took flat conformations within the remaining phase I layer of water. In this way the PEO blocks acted as effective anchors and after a certain point dominated over the small number of PI blocks. Nevertheless, at the same time the hydrophobic PI blocks came together in order to minimize the area of contact with the unfavorable air and water, forming a "small" assembly. The low height (≈0.4 nm) areas (green) of the substructure can be associated with the laterally extended PEO blocks within/on the phase I water layer while the 1 nm height areas (red) can be associated with the small PI block aggregates (Figure 6h). The difference of behavior between the large polymer islands which incorporate many chains (originating from few to several micelles) and the small polymer islands which incorporate fewer chains (originating from accumulation of free chains and/or parts of micelles) is tentatively attributed to a competition between the anchoring behavior of the PEO blocks within the phase I water on mica and the clustering behavior of PI blocks on top, indicating the existence of a specific "threshold" number of polymer chains below which the PEO anchors dominate over the PI clustering while above this number the PI clustering dominate over the PEO anchors. It is to be expected that this threshold number will depend not only on the strength of the relevant interactions but also on the lengths of the two blocks and can provide opportunities for fabrication of smart/responsive surfaces.

Our system cannot be considered reversible as the mica changes its properties permanently with time (it becomes less hydrophilic). It has been recently shown that the irreversibly adsorbed hydrophilic polymers on mica can act as molecular templates leading to interesting "nanodomain memory" effects.[74] Furthermore, from our observations we can deduce the essential ingredients for the design of controlled surface nanostructures and surfaces of tunable roughness/shape: (i) surfaces acting as substrates that can alter their hydrophilicity upon the change of an external stimulus such as electric potential or light in combination with (ii) amphiphilic block copolymers consisting of a hydrophilic block and a highly flexible hydrophobic block. We expect that these results can be generalized to a wide range of surfaces and functional materials and can be used to develop controlled nanostructures and smart responsive surfaces.

Conclusions

The time-dependent evolution of the shape and height of the PI−PEO block copolymer modified mica in ambient conditions was observed by atomic force microscopy. The PI−PEO micelles deposited on mica dissociated forming ultrathin, flat polymer islands which were partly adsorbed and partly floating on the substrate. Furthermore, they showed an exponential-type growth of height with time. The AFM images revealed that during this growth the lateral shape of the initially flat polymer structures changed gradually from asymmetric/irregular to circular. The observed phenomena were driven by the change of mica from strongly hydrophilic to less hydrophilic with increasing exposure to air in ambient conditions. During this change the initial mobile water layer of phase II evaporated, resulting in the gradual formation of large central globular aggregates of mainly PI blocks on top of PEO blocks or parts of PEO blocks firmly attached on the mica surface. The behavior of smaller structures was different as they laterally expanded and became shorter with time. In this case, the PEO blocks anchoring dominated over the PI clustering and the central small aggregate became shorter.

Acknowledgment. We thank Christopher Hall, Michael Zaiser, Neil Thomson, and George Fytas for fruitful discussions. This work was supported by the EPSRC DTA and the Institute of Materials and Processes, School of Engineering and Electronics at the University of Edinburgh.

References and Notes

(1) Cheng, J. Y.; Ross, C. A.; Smith, H. I.; Thomas, E. L. *Adv. Mater.* **2006**, *18* (19), 2505–2521.
(2) Park, C.; Yoon, J.; Thomas, E. L. *Polymer* **2003**, *44* (22), 6725–6760.
(3) Segalman, R. A. *Mater. Sci. Eng.: R: Rep.* **2005**, *48* (6), 191–226.
(4) Khor, H. L.; Kuan, Y.; Kukula, H.; Tamada, K.; Knoll, W.; Moeller, M.; Hutmacher, D. W. *Biomacromolecules* **2007**, *8* (5), 1530–1540.
(5) Glass, R.; Möller, M.; Spatz, J. P. *Nanotechnology* **2003**, *14* (10), 1153–1160.
(6) Webber, G. B.; Wanless, E. J.; Armes, S. P.; Tang, Y.; Li, Y.; Biggs, S. *Adv. Mater.* **2004**, *16* (20), 1794–1798.
(7) Webber, G. B.; Wanless, E. J.; Butun, V.; Armes, S. P.; Biggs, S. *Nano Lett.* **2002**, *2* (11), 1307–1313.
(8) Xu, C.; Fu, X.; Fryd, M.; Xu, S.; Wayland, B. B.; Winey, K. I.; Composto, R. J. *Nano Lett.* **2006**, *6* (2), 282–287.
(9) Spatz, J. P.; Sheiko, S.; Möller, M. *Adv. Mater.* **1996**, *8* (6), 513–517.
(10) Spatz, J. P.; Möller, M.; Noeske, M.; Behm, R. J.; Pietralla, M. *Macromolecules* **1997**, *30* (13), 3874–3880.
(11) Spatz, J. P.; Eibeck, P.; Mössmer, S.; Möller, M.; Kramarenko, E. Y.; Khalatur, P. G.; Potemkin, I. I.; Khokhlov, A. R.; Winkler, R. G.; Reineker, P. *Macromolecules* **2000**, *33* (1), 150–157.
(12) Lu, C.; Guo, S.; Liu, L.; Zhang, Y.; Li, Z.; Gu, J. *J. Polym. Sci., Part B: Polym. Phys.* **2006**, *44* (23), 3406–3417.
(13) Li, F.; Balastre, M.; Schorr, P.; Argillier, J. F.; Yang, J.; Mays, J. W.; Tirrell, M. *Langmuir* **2006**, *22* (9), 4084–4091.
(14) Sakai, K.; Smith, E. G.; Webber, G. B.; Schatz, C.; Wanless, E. J.; Butun, V.; Armes, S. P.; Biggs, S. *Langmuir* **2006**, *22* (12), 5328–5333.
(15) Zhao, J.; Tian, S.; Wang, Q.; Liu, X.; Jiang, S.; Ji, X.; An, L.; Jiang, B. *Eur. Phys. J. E* **2005**, *16* (1), 49–56.
(16) Chen, Y.; Huang, H.; Hu, Z.; He, T. *Langmuir* **2004**, *20* (9), 3805–3808.
(17) Kago, K.; Matsuoka, H.; Yoshitome, R.; Mouri, E.; Yamaoka, H. *Langmuir* **1999**, *15* (12), 4295–4301.
(18) Meiners, J. C.; Ritzi, A.; Rafailovich, M. H.; Sokolov, J.; Mlynek, J.; Krausch, G. *Appl. Phys. A* **1995**, *61* (5), 519–524.
(19) Meiners, J. C.; Quintel-Ritzi, A.; Mlynek, J.; Elbs, H.; Krausch, G. *Macromolecules* **1997**, *30* (17), 4945–4951.
(20) Stamouli, A.; Pelletier, E.; Koutsos, V.; van der Vegte, E.; Hadziioannou, G. *Langmuir* **1996**, *12* (13), 3221–3224.
(21) Talingting, M. R.; Ma, Y.; Simmons, C.; Webber, S. E. *Langmuir* **2000**, *16* (2), 862–865.
(22) Webber, G. B.; Wanless, E. J.; Armes, S. P.; Baines, F. L.; Biggs, S. *Langmuir* **2001**, *17* (18), 5551.
(23) Hamley, I. W.; Connell, S. D.; Collins, S. *Macromolecules* **2004**, *37* (14), 5337–5351.
(24) Connell, S. D.; Collins, S.; Fundin, J.; Yang, Z.; Hamley, I. W. *Langmuir* **2003**, *19* (24), 10449–10453.
(25) Potemkin, I. I.; Kramarenko, E. Y.; Khokhlov, A. R.; Winkler, R. G.; Reineker, P.; Eibeck, P.; Spatz, J. P.; Moller, M. *Langmuir* **1999**, *15* (21), 7290–7298.
(26) Hamley, I. W. *The Physics of Block Copolymers*; Oxford University Press: New York, 1999.
(27) Hadjichristidis, N.; Pispas, S.; Floudas, G. *Block Copolymers: Synthetic Strategies, Physical Properties, and Applications*; Wiley-Interscience: Hoboken, NJ, 2002.
(28) Ligoure, C. *Macromolecules* **1991**, *24* (10), 2968–2972.
(29) Alexandridis, P., Lindman, B., Eds. *Amphiphilic Block Copolymers. Self-Assembly and Applications*; Elsevier: Amsterdam, 2000.
(30) Pispas, S.; Hadjichristidis, N. *Langmuir* **2003**, *19* (1), 48–54.
(31) Toomey, R.; Mays, J.; Yang, J.; Tirrell, M. *Macromolecules* **2006**, *39* (6), 2262–2267.
(32) Langmuir, I. *J. Am. Chem. Soc.* **1918**, *40* (9), 1361–1403.

(33) Brunauer, S. *The Adsorption of Gases and Vapors*; Oxford University Press: London, 1943.
(34) Israelachvili, J.; Pashley, R. *Nature (London)* **1982**, *300* (5890), 341–342.
(35) Hu, J.; Xiao, X.-d.; Ogletree, D. F.; Salmeron, M. *Science* **1995**, *268* (5208), 267–269.
(36) Hu, J.; Xiao, X.-d.; Ogletree, D. F.; Salmeron, M. *Surf. Sci.* **1995**, *344* (3), 221–236.
(37) Cantrell, W.; Ewing, G. E. *J. Phys. Chem. B* **2001**, *105* (23), 5434–5439.
(38) Spagnoli, C.; Loos, K.; Ulman, A.; Cowman, M. K. *J. Am. Chem. Soc.* **2003**, *125* (23), 7124–7128.
(39) Cheng, L.; Fenter, P.; Nagy, K. L.; Schlegel, M. L.; Sturchio, N. C. *Phys. Rev. Lett.* **2001**, *87* (15), 156103/1–156103/4.
(40) Beaglehole, D.; Christenson, H. K. *J. Phys. Chem.* **1992**, *96* (8), 3395–3403.
(41) Park, S.-H.; Sposito, G. *Phys. Rev. Lett.* **2002**, *89* (8), 085501/1–085501/3.
(42) Odelius, M. *Phys. Rev. Lett.* **1999**, *82* (19), 3919–3922.
(43) Thomson, N. H. *J. Microsc. (Oxford, U.K.)* **2005**, *217* (3), 193–199.
(44) Crampton, N.; Bonass, W. A.; Kirkham, J.; Thomson, N. H. *Langmuir* **2005**, *21* (17), 7884–7891.
(45) Crampton, N.; Bonass, W. A.; Kirkham, J.; Thomson, N. H. *Ultramicroscopy* **2006**, *106* (8−9), 765–770.
(46) Kumaki, J.; Hashimoto, T. *J. Am. Chem. Soc.* **2003**, *125* (16), 4907–4917.
(47) Kumaki, J.; Nishikawa, Y.; Hashimoto, T. *J. Am. Chem. Soc.* **1996**, *118* (13), 3321–3322.
(48) Kumaki, J. *Macromolecules* **1988**, *21* (3), 749–755.
(49) Hadjichristidis, N.; Iatrou, H.; Pispas, S.; Pitsikalis, M. *J. Polym. Sci., Part A: Polym. Chem.* **2000**, *38* (18), 3211–3234.
(50) Uhrig, D.; Mays, J. W. *J. Polym. Sci., Part A: Polym. Chem.* **2005**, *43* (24), 6179–6222.
(51) Esswein, B.; Möller, M. *Angew. Chem., Int. Ed. Engl.* **1996**, *35* (6), 623–625.
(52) Förster, S.; Krämer, E. *Macromolecules* **1999**, *32* (8), 2783–2785.
(53) Magonov, S. N.; Elings, V.; Whangbo, M. H. *Surf. Sci.* **1997**, *375* (2−3), L385−L391.
(54) Magonov, S. N.; Reneker, D. H. *Annu. Rev. Mater. Sci.* **1997**, *27*, 175–222.
(55) Godehardt, R.; Lebek, W.; Adhikari, R.; Rosenthal, M.; Martin, C.; Frangov, S.; Michler, G. H. *Eur. Polym. J.* **2004**, *40* (5), 917–926.
(56) Koutsos, V.; van der Vegte, E. W.; Grim, P. C. M.; Hadziioannou, G. *Macromolecules* **1998**, *31* (1), 116–123.
(57) Krishnamoorti, R.; Graessley, W. W.; Zirkel, A.; Richter, D.; Hadjichristidis, N.; Fetters, L. J.; Lohse, D. J. *J. Polym. Sci., Part B: Polym. Phys.* **2002**, *40* (16), 1768–1776.
(58) Bliznyuk, V. N.; Assender, H. E.; Briggs, G. A. D. *Macromolecules* **2002**, *35* (17), 6613–6622.
(59) Štěpánek, M.; Humpolíčkova, J.; Procházka, K.; Hof, M.; Tuzar, Z.; Špírkova, M.; Wolff, T. *Collect. Czech. Chem. Commun.* **2003**, *68* (11), 2120–2138.
(60) Matějíček, P.; Humpolíčkova, J.; Prochaázka, K.; Tuzar, Z.; Špírkova, M.; Hof, M.; Webber, S. E. *J. Phys. Chem. B* **2003**, *107* (32), 8232–8240.
(61) Vaia, R. A.; Vasudevan, S.; Krawiec, W.; Scanlon, L. G.; Giannelis, E. P. *Adv. Mater.* **1995**, *7* (2), 154–156.
(62) Hackett, E.; Manias, E.; Giannelis, E. P. *Chem. Mater.* **2000**, *12* (8), 2161–2167.
(63) Elmahdy, M. M.; Chrissopoulou, K.; Afratis, A.; Floudas, G.; Anastasiadis, S. H. *Macromolecules* **2006**, *39* (16), 5170–5173.
(64) Krishnamoorti, R.; Vaia, R. A.; Giannelis, E. P. *Chem. Mater.* **1996**, *8* (8), 1728–1734.
(65) Vaia, R. A.; Sauer, B. B.; Tse, O. K.; Giannelis, E. P. *J. Polym. Sci., Part B: Polym. Phys.* **1997**, *35* (1), 59–67.
(66) Kuppa, V.; Menakanit, S.; Krishnamoorti, R.; Manias, E. *J. Polym. Sci., Part B: Polym. Phys.* **2003**, *41* (24), 3285–3298.
(67) Kuppa, V.; Manias, E. *Chem. Mater.* **2002**, *14* (5), 2171–2175.
(68) Kuppa, V.; Manias, E. *J. Chem. Phys.* **2003**, *118* (7), 3421–3429.
(69) Strawhecker, K. E.; Manias, E. *Chem. Mater.* **2003**, *15* (4), 844–849.
(70) Roiter, Y.; Minko, S. *J. Am. Chem. Soc.* **2005**, *127* (45), 15688–15689.
(71) Poppe, A.; Willner, L.; Allgaier, J.; Stellbrink, J.; Richter, D. *Macromolecules* **1997**, *30* (24), 7462–7471.
(72) Smith, G. D.; Yoon, D. Y.; Jaffe, R. L.; Colby, R. H.; Krishnamoorti, R.; Fetters, L. J. *Macromolecules* **1996**, *29* (10), 3462–3469.
(73) Glynos, E.; Chremos, A.; Petekidis, G.; Camp, J. P.; Koutsos, V. *Macromolecules* **2007**, *40* (19), 6947–6958.
(74) Pelah, A.; Luduena, S. J.; Jares-Erijman, E. A.; Szleifer, I.; Pietrasanta, L. I.; Jovin, T. M. *Langmuir* **2006**, *22* (23), 9682–9686.

MA702630C